

The Evolution of Galaxy Clustering in Hierarchical Models

Shaun Cole, Andrew Benson, Carlton Baugh, Cedric Lacey and Carlos Frenk.

Department of Physics, University of Durham, South Road, Durham, DH1 3LE U.K.

Abstract. The main ingredients of recent semi-analytic models of galaxy formation are summarised. We present predictions for the galaxy clustering properties of a well specified Λ CDM model whose parameters are constrained by observed local galaxy properties. We present preliminary predictions for evolution of clustering that can be probed with deep pencil beam surveys.

1. Introduction

Observations now probe the properties of galaxy populations over a large fraction of the age of the universe (e.g. Steidel et al. 1996; Ellis et al. 1996; Lilly et al. 1996; Adelberger et al. 1998). Furthermore, we can look forward to a much more detailed study of the high redshift universe with the many instruments soon to be commissioned on the growing generation of new 8-m class telescopes. Over the lookback time probed by these observations the conventional cold dark matter dominated models of structure formation predict very strong evolution of the distribution of dark matter. It is therefore the job of theorists to progress to the stage where these observations can be interpreted and further properties predicted within the framework of the hierarchical evolution of dark matter halos.

The main approaches that have been taken towards this goal can be divided into two classes. The first, direct simulation, involves solving explicitly the gravitational and hydrodynamical equations in the expanding universe using numerical N-body techniques (e.g. Katz et al. 1992; Evrard et al. 1994; Navarro & Steinmetz 1997; Frenk et al. 1999; Pearce et al. 1999). The second approach, now commonly known as “semi-analytic modelling of galaxy formation”, calculates the evolution of the baryonic component using simple analytic models, and uses a Monte-Carlo technique to generate merger trees that describe the hierarchical growth of dark matter halos.

The two modelling techniques have complementary strengths. The major advantage of direct simulations is that the dynamics of the cooling gas are calculated in full generality, without the need for simplifying assumptions. The main disadvantage is that even with the best codes and fastest computers available, the attainable resolution is still some orders of magnitude below that required to fully resolve the formation and internal structure of individual galaxies in cosmological volumes. In addition, a phenomenological model, similar to that employed in semi-analytic models, is required to include star formation and feedback processes. Semi-analytic models do not suffer from such resolution limitations. Their major disadvantage is the need for simplifying assumptions

in the calculation of gas properties, such as spherical symmetry which is imposed to estimating the cooling rate of halo gas. An important advantage of semi-analytic models is their flexibility, which allows the effects of varying assumptions or parameter choices to be readily investigated and makes it possible to calculate a wide range of observable galaxy properties, such as luminosities, sizes, mass-to-light ratios, bulge-to-disk ratios, circular velocities, etc.

Semi-analytic models of galaxy formation based on Monte-Carlo methods for generating halo merger trees were pioneered by two groups, one now based in Munich (e.g. Kauffmann, White & Guiderdoni 1993; Kauffmann & Charlot 1994; Kauffmann 1995a,b; Diaferio et al. 1999) and the other in Durham (e.g. Cole et al. 1994; Baugh et al. 1998; Governato et al. 1998; Benson et al. 1999a,b; Cole et al. 1999). There is now a third, well established independent group (Somerville & Primack 1999; Somerville & Kolatt 1999; Somerville et al. 1999) and the field continues to grow with interesting variants being developed, for example, by Roukema et al. (1997), Avila-Reese & Firmani (1998), Wu, Fabian & Nulsen (1998) and van Kampen, Jimenez & Peacock (1999). The numerous contributions of these groups to this meeting are an indication of the versatility and usefulness of this approach to modelling galaxy formation.

There are typically a large number of differences between the detailed assumptions made in any two of the above models. Many of these relate to the prescription for generating the halo merger trees. These differences typically have little effect on model predictions. Also one can expect this aspect of the various approaches to converge, because in each case the models are attempting to emulate the evolution of dark matter halos seen in high resolution N-body simulations. The most important differences relate to assumptions regarding star formation, e.g. the importance of merger induced bursts and the manner in which stellar feedback operates. In this respect all the models are, inevitably, oversimplified and probably the best way forward is to confront the models continually with ever more detailed and accurate data. The great value of the semi-analytic approach is its ability to address a wide range of observational data from galaxy luminosity functions, colour and metallicity distributions to clustering statistics within a single coherent model. We have found this to be a particular strength of the models as it often allows robust predictions to be made despite the intrinsic uncertainty in the physical processes that are being modelled.

In the remainder of this article we briefly describe the latest Durham model and use it to illustrate the main processes that are incorporated in semi-analytic models of galaxy formation. We then present a comprehensive set of results for the galaxy clustering properties predicted by this model for a Λ CDM ($\Omega_0 = 0.3$, $\Lambda_0 = 0.7$) cosmology, after the model is constrained to reproduce the the bright end of the observed galaxy luminosity function.

2. The Model

A full description of the current Durham semi-analytic galaxy formation model, complete with an exploration of how the predictions depend on parameter variations and how they compare to observational data, can be found in Cole et al. (1999). Here we simply describe the main features of the model.

2.1. Merger Trees

We use a simple new Monte-Carlo algorithm to generate merger trees that describes the formation paths of randomly selected dark matter halos. Our algorithm is based directly on the analytic expression for halo merger rates derived by Lacey & Cole (1993). The algorithm enables the merger process to be followed with high time resolution, as timesteps are not imposed on the tree but rather are controlled directly by the frequency of mergers. Also, there is no quantization of the masses of the halos.

2.2. Halo Structure and Gas Cooling

We assume that the dark matter in virialized halos is well described by the NFW density profile (Navarro, Frenk & White 1997). We further assume that any diffuse gas present during a halo merger is shock-heated to the virial temperature of the halo. The density profile we adopt for the hot gas is less centrally concentrated than that of the dark matter and is chosen to be in agreement with the results of high resolution simulations of non-radiative gas (e.g. Frenk et al. 1999). We estimate the fraction of gas that can cool in a halo by computing the radius at which the radiative cooling time of the gas equals the age of the halo. The gas that cools is assumed to conserve angular momentum and settle into a rotationally supported disk. Thus, the initial angular momentum of the halo, which we assign using the well characterised distribution of spin parameters found for halos in N-body simulations, determines the size of the resulting galaxy disk. In computing the size of the disk we also take account of the contraction of the inner part of the halo caused by the gravity of the disk.

2.3. Star Formation and Feedback

The processes of star formation and stellar feedback are the most uncertain to model. We adopt a flexible approach in which the star formation rate in the disk of cold gas is given by $\dot{M}_\star = M_{\text{cold}}/\tau_\star$, with the timescale τ_\star parameterized as

$$\tau_\star = \epsilon_\star^{-1} \tau_{\text{disk}} (V_{\text{disk}}/200 \text{ km s}^{-1})^{\alpha_\star}. \quad (1)$$

We also adopt a feedback model in which for every solar mass of stars formed,

$$\beta = (V_{\text{disk}}/V_{\text{hot}})^{-\alpha_{\text{hot}}} \quad (2)$$

solar masses of gas are assumed to be reheated and ejected from the disk as a result of energy input from young stars and supernovae. In these formulae, τ_{disk} and V_{disk} are the dynamical time and circular velocity of the disk; ϵ_\star , α_\star , α_{hot} and V_{hot} are the model parameters.

2.4. Galaxy Mergers

Mergers between galaxies can occur, subsequent to the merger of their dark matter halos, if dynamical friction causes the orbits of the galaxies to decay. The result of a merger depends on the mass ratio of the merging galaxies. If they are comparable, $M_{\text{smaller}} > f_{\text{ellip}} M_{\text{larger}}$, then the merger is said to be violent and results in the formation of a spheroid. At this point any cold gas present in the merger is assumed to undergo a burst of star formation, with a timescale

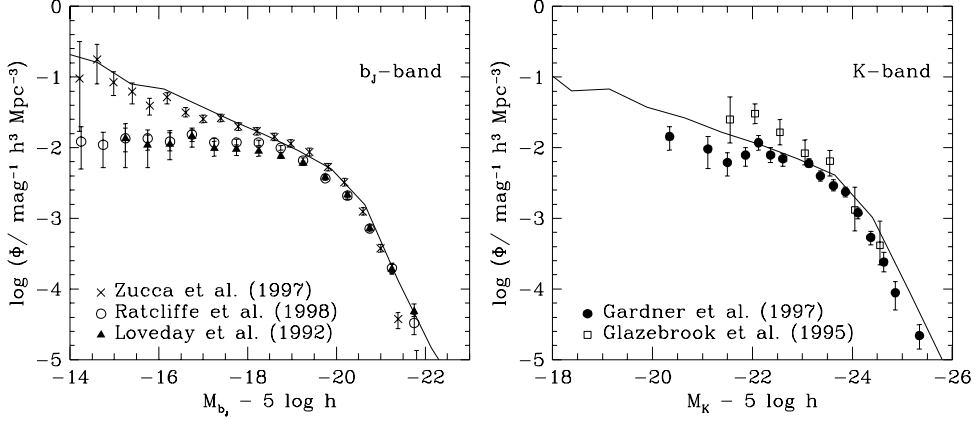


Figure 1. The b_J and K-band luminosity functions of our Λ CDM model compared to a variety of observational estimates (symbols).

equal to the dynamical time of the forming spheroid and with feedback estimated using equation (2), but with the circular velocity of the spheroid replacing that of the disk. The size of the resulting spheroid is estimated assuming energy conservation in the merger (once dynamical friction has eroded the orbits to the point where the galaxies interpenetrate) and the virial theorem. For minor mergers, $M_{\text{smaller}} < f_{\text{ellip}} M_{\text{larger}}$, we assume the cold gas is accreted by the disk and the stars by the bulge of the larger galaxy.

2.5. Stellar Population Synthesis and Dust

To convert the calculated star formation histories of each galaxy into observable luminosities and colours we use the stellar population synthesis model of Bruzual & Charlot (1993,1999) and, in addition, the 3-dimensional dust model of Ferrara et al. (1999). For the former we adopt the IMF of the solar neighbourhood as parameterized by Kennicutt (1983) and for the latter we adopt their Milky Way extinction law and assume that the dust/gas ratio in the cold gas disk scales with metallicity.

2.6. Galaxy Clustering

Given a list of halo masses, at the present day or at some redshift z , the above model can be used to determine the number, luminosity and other properties of the galaxies that inhabit them. It is then straightforward to compute the amplitude of their correlation function on large scales using the formalism of Mo & White (1996). Here we use a more direct approach, that of using the positions of halos from an N-body simulation, as this enables the correlation function to be studied down to smaller scales and allows other aspects of galaxy clustering to be investigated. Details of our procedure can be found in Benson et al. (1999a).

3. Observational Constraints

The number of parameters in our galaxy formation model is not small and the intrinsic range of behaviour that the model can produce is large. This is in-

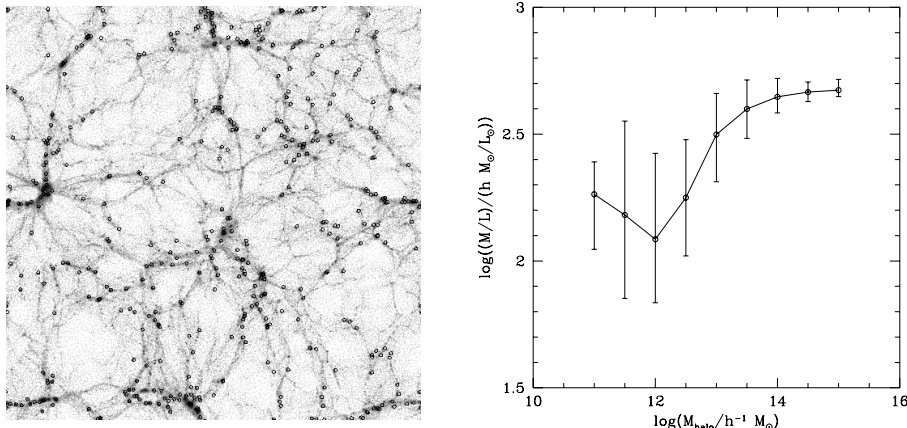


Figure 2. The left hand panel shows a $141 \times 141 \times 8h^{-3}\text{Mpc}^3$ slice of the ΛCDM dark matter simulation with the positions of galaxies brighter than $M_B - 5\log h = -19.5$ overlaid. The right hand panel shows the variation of the total mass-to-light ratio of halos as a function of mass.

evitable as galaxy formation, at the very least, involves all the processes which are included in the model and quite possibly others as well. Thus, progress can only be made if a set of constraints is applied to fix model parameters. Our approach, set out in detail in Cole et al. (1999), is to fix these parameters using the observed properties of the local galaxy population, e.g. the B and K-band luminosity functions, the slope of the Tully-Fisher relation and the gas fractions and metallicities of disk galaxies. The result of applying these constraints is a well specified model whose properties can be examined and critically compared to other observational data such as galaxy clustering or high redshift observations.

Fig. 1 shows the b_J and K-band luminosity functions of a ΛCDM model ($\Omega_0 = 0.3$, $\Lambda_0 = 0.7$) constrained in this way. It turns out that the predicted low redshift galaxy clustering is insensitive to changes in the model parameters provided only that the model is constrained to produce a reasonable match to the bright end of the luminosity function (Benson et al. 1999a).

4. Results

We now look at a variety of clustering properties that we predict for the constrained ΛCDM model and compare them with available observational data. The N-body simulation used to assign positions to our galaxies is the ΛCDM “GIF” simulation carried out by the Virgo consortium.

These same simulations have been analyzed in great detail by the Munich group, with results presented at this meeting and in Kauffmann et al. (1999a,b) and Diaferio et al. (1999). Their approach is more sophisticated than ours in that they extract the halo merger trees directly from the N-body simulations and are able to follow individual galaxies in the simulation from one epoch to another. However, these differences in approach do not significantly affect the predictions of the clustering and kinematic properties of the galaxy populations.

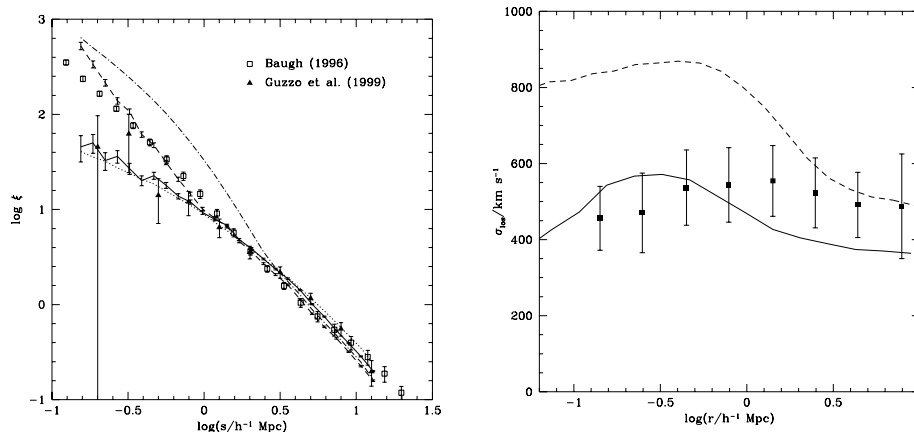


Figure 3. The left hand panel shows real/redshift space correlations functions of the dark matter (dot-dashed/dotted) and galaxies (dashed/solid) and also observational estimates of the real and redshift space galaxy correlation function. The right panel shows the pairwise velocity dispersion, σ_{los} , of dark matter (broken line) and galaxies (solid line) and an observational estimate from the LCRS (Jing, Mo & Borner 1998).

In particular, with Antonaldo Diaferio, we were able to verify that if we use our algorithm to assign galaxies positions, but start with the Munich group's list of galaxies as a function of halo mass, we recover very similar results to those reported in Diaferio et al. (1999). These tests are discussed in Benson et al. (1999b), where we conclude that in the few cases where significant differences exist between our results and those of the Munich group, they are largely a result of the differing constraints that have been applied to the models.

4.1. Low Redshift Clustering

We start, in Fig. 2a, by showing a slice through the N-body simulation with the positions of galaxies superimposed on the dark matter distribution. It is worth noting that the way in which galaxies trace the dark matter is non-trivial with galaxies avoiding the large underdense regions and concentrating in filaments and clusters. In our model this distribution is entirely determined by the combination of the dark matter distribution and the distribution of the number of galaxies within halos as a function of halo mass. One representation of this distribution is Fig. 2b, which shows the variation of total mass-to-light ratio of halos as a function of halo mass, with the errorbars indicating the 10 and 90 centiles of this distribution. This dependence is produced naturally by the physics incorporated into the semi-analytic model. Galaxy formation is most efficient (M/L lowest) in intermediate mass halos. The efficiency is reduced in low mass halos due to feedback and in the most massive halos due to long cooling times. The low efficiency in low mass halos leads to the production of large voids in the galaxy distribution, while the inefficiency at high masses leads to an anti-bias in small scale clustering, as shown by the real-space correlation functions of Fig. 3a. In fact the real-space galaxy correlation function has a nearly power law form in

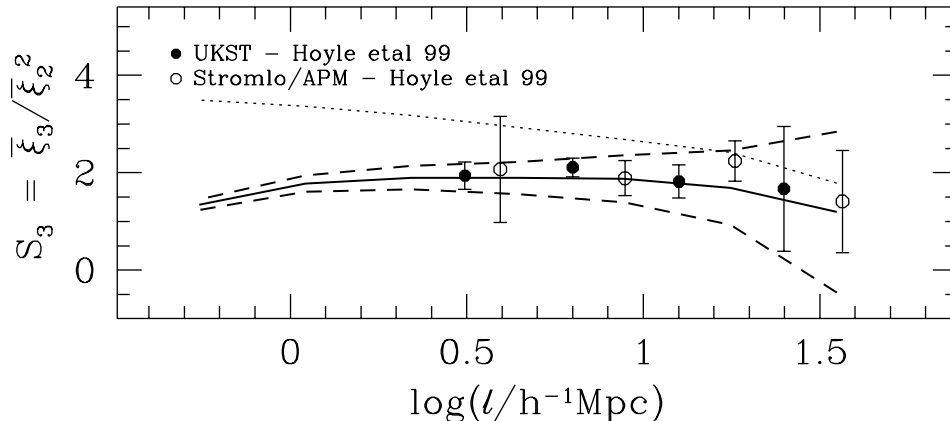


Figure 4. The skewness, S_3 , of the distribution of counts in cubical cells in redshift space as a function cell size. The dotted line shows S_3 for the dark matter and the solid line S_3 for the galaxies. The dashed lines show the $1\text{-}\sigma$ uncertainty in this estimate. The points with errorbars show two recent observational estimates.

quite good agreement with that observed. The underrepresentation of galaxies in clusters also leads to a reduced pairwise velocity dispersion (Fig. 3b) which is close to the observed value. Strangely, the different dark matter and galaxy peculiar velocities act to produce very similar redshift space correlation functions for both components and these match well the observed redshift-space galaxy correlation function.

Fig. 4 compares the skewness, S_3 , in redshift space as a function of cell size with two recent observational estimates. The skewness of the model galaxy distribution is substantially less than that of the dark matter and in remarkably good agreement with the observed values.

4.2. The Evolution of galaxy clustering

A strong test of the models will come from comparing their predictions against high redshift observations. One highly successful comparison has already been made. In Baugh et al. (1998) and Governato et al. (1998) firm predictions for the Lyman-break galaxy correlation function were made. These later proved to agree remarkably well with observations (Adelberger et al. 1998). Unfortunately the predictions for both low and high Ω_0 models are very similar and so the observations do not discriminate between cosmological models.

In order to make detailed comparisons of the galaxy formation models with the ever increasing quantity of high redshift data we are developing techniques to simulate deep pencil beam surveys and accurately match observational selection criteria. Fig. 5 shows a simulated deep R-band image constructed using our technique of outputting a light-cone from an evolving N-body simulation and then using the semi-analytic galaxy formation model to populate its halos with galaxies. Given the limited resolution and volume of the simulation used to construct these prototypes one should be somewhat cautious to avoid over-interpreting their predictions. Nevertheless it is interesting to make a preliminary comparison with some recent observations.

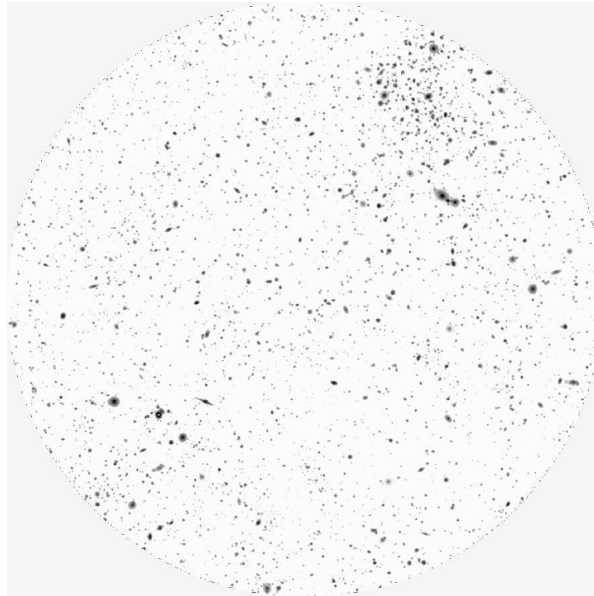


Figure 5. A mock image of a 18 arc minute diameter field to a limiting magnitude of $R=24$ constructed from a simulated light-cone.

Fig. 6 compares predictions for the clustering amplitude at one degree as a function of limiting K-magnitude and for redshift slices. The model predictions are based on an ensemble of simulated light cones with the errorbars indicating the rms scatter. The model agrees well with the K-band observations of McCracken (1999). The model predicts very little variation of clustering amplitude with redshift, whereas Magliocchetti & Maddox (1999) find quite a strong trend. However, the errorbars are large and larger area surveys will be required to critically test the models.

5. Conclusions

Physically motivated semi-analytic models of galaxy formation which, importantly, include the evolution of structure, provide a framework in which very diverse properties of galaxies can be modelled and understood. Using a subset of the locally observed galaxy properties these models can be constrained and then employed to make useful predictions. Such predictions include all aspects of galaxy evolution and also galaxy clustering.

We have only examined the predicted clustering properties for a couple of cosmological models (Benson et al. 1999a). However, it is intriguing that the results of the Λ CDM model presented here appear to match galaxy clustering data remarkably well and significantly better than a τ CDM model.

We have invested in the technology necessary to extend the model predictions to high redshift by simulating deep pencil beams. Soon, such data will provide very interesting tests of galaxy formation models.

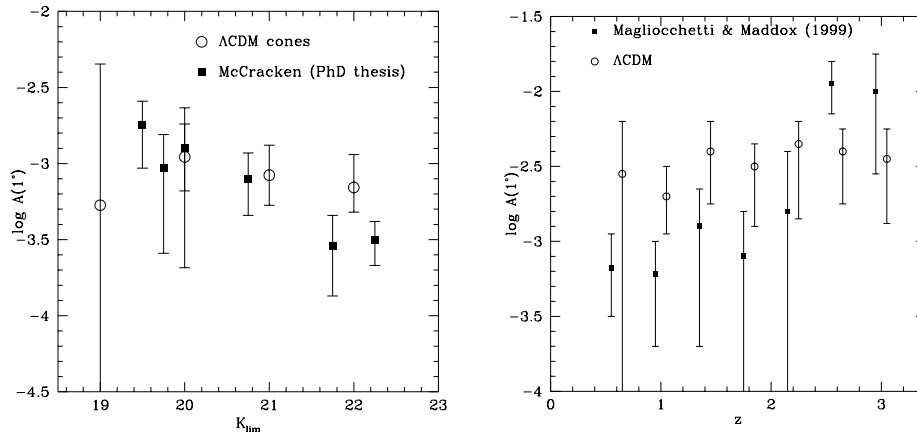


Figure 6. The model prediction for the dependence of the amplitude at one degree of the angular correlation function $w(\theta)$ versus a) limiting K-band magnitude and b) redshift. In each case the selection criteria were chosen to mimic those of the observational dataset with which they are compared.

References

- Adelberger, K.L., Steidel, C.C., Giavalisco, M., Dickinson, M., Pettini, M., Kellogg, M. 1998, *ApJ*, 505, 1
- Avila-Reese, V., Firmani, C. 1998, *ApJ*, 505, 37
- Baugh, C.M. 1996, *MNRAS*, 280, 267
- Baugh, C.M., Cole, S., Frenk, C.S., Lacey, C.G. 1998, *ApJ*, 498, 504
- Benson, A.J., Cole, S., Frenk, C.S., Baugh, C.M., Lacey, C.G. 1999a, *MNRAS*, in press.
- Benson, A.J., Cole, S., Baugh, C.M., Frenk, C.S., Lacey, C.G. 1999b, *MNRAS*, submitted.
- Bruzual, A.G., Charlot, S. 1993, *ApJ*, 405, 538
- Bruzual, A.G., Charlot, S. 1999, in preparation.
- Cole, S., Aragón-Salamanca, A., Frenk, C.S., Navarro, J.F., Zepf, S.E. 1994, *MNRAS*, 271, 781
- Cole, S., Lacey, C.G., Baugh, C.M., Frenk C.S. 1999, *MNRAS*, submitted.
- Diaferio, A. Kauffmann, G., Colberg, J.M., White, S.D.M. 1999, *MNRAS*, 307, 537
- Ellis, R.S., Colless, M., Broadhurst, T., Heyl, J., Glazebrook, K. 1996, *MNRAS*, 285, 613
- Evrard, A.E. Summers, F., Davis, M. 1994, *ApJ*, 422, 11
- Ferrara, A., Bianchi, S., Cimatti, A., Giovanardi C. 1999, *ApJS*, 123, 437
- Frenk, C.S., et al. 1999, *ApJ*, in press.
- Gardner, J.P., Sharples, R.M., Frenk, C.S., Carrasco, B.E. 1997, *ApJ*, 480, L99
- Glazebrook, K., Peacock, J.A., Miller, L., Collins, C.A. 1995, *MNRAS*, 275, 169

- Governato, F., Baugh, C.M., Frenk, C.S., Cole, S., Lacey, C.G., Quinn, T., Stadel, J. 1998, *Nature* 392, 359
- Guzzo et al. 1999 (astro-ph/9901378)
- Hoyle, F., Szapudi, I., Baugh, C.M. 1999, *MNRAS*, submitted.
- Jing, Y.P., Mo, H.J., Borner, G. 1998, *ApJ*, 494, L1
- van Kampen E., Jimenez, J., Peacock, J.A. 1999, *MNRAS*, submitted.
- Katz, N., Hernquist, L., Weinberg D.H. 1992, *ApJ*, 399, L109
- Kauffmann, G. 1995a, *MNRAS*, 274, 153
- Kauffmann, G. 1995b, *MNRAS*, 274, 161
- Kauffmann, G., White, S.D.M., Guiderdoni, B. 1993, *MNRAS*, 264, 201
- Kauffmann, G., Charlot, S. 1994, *ApJ*, 430, L97
- Kauffmann, G., Colberg, J.M., Diaferio, A., White, S.D.M. 1999a, *MNRAS*, 303, 188
- Kauffmann, G., Colberg, J.M., Diaferio, A., White, S.D.M. 1999b, *MNRAS*, 307, 529
- Kennicutt, R.C. 1983, *ApJ*, 272, 54
- Lacey, C.G., Cole, S. 1993, *MNRAS*, 262, 627
- Lilly, S.J., Le Fevre, O., Hammer, F. Crampton, D. 1996, *ApJ*, 460, 1
- Loveday, J., Peterson, B. A., Efstathiou, G., Maddox, S.J. 1992, *ApJ*, 90, 338
- Magliocchetti, M., Maddox, S.J. 1999, *MNRAS*, 306, 998
- McCracken, H.J. 1999, Ph.D thesis, University of Durham
- Mo, H.J., White, S.D.M. 1996, *MNRAS*, 282, 347
- Navarro, J.F., Frenk, C.S., White, S.D.M. 1997, *ApJ*, 490, 493
- Navarro, J.F., Steinmetz, M. 1997, *ApJ*, 478, 13
- Pearce, F.R., Jenkins, A., Frenk, C.S., Colberg, J.M., White, S.D.M., Thomas, P.A., Couchman, H.M.P, Peacock, J.A., Efstathiou, G. 1999, *ApJ*, 521, L9
- Ratcliffe, A., Shanks, T., Parker, Q.A., Fong, R. 1998, *MNRAS*, 294, 147
- Roukema, B.F., Peterson, B.A. Quinn, P.J., Rocca-Volmerange, B. 1997, *MNRAS*, 292, 835
- Somerville, R.S., Kolatt, T.S. 1999, *MNRAS*, 305, 1
- Somerville, R.S., Lemson, G., Kolatt, T.S., Dekel, A. 1999, *MNRAS*, submitted (astro-ph/9807277)
- Somerville, R.S., Primack, J.R. 1999, *MNRAS*, in press (astro-ph/9802268)
- Steidel, C.C., Giavalisco, M., Pettini, M., Dickinson, M., Adelberger, K.L. 1996, *ApJ*, 462, 17
- Wu, K.K.S., Fabian, A.C., Nulsen, P.E.J. 1998, *MNRAS*, 301, L20
- Zucca, E., et al. 1997, *A&A*, 326, 477